Percolative metal-insulator transition in $LaMnO_3$

M. Sherafati,[1,*] M. Baldini,[2,3] L. Malavasi,[4] and S. Satpathy[1]

[1]*Department of Physics & Astronomy, University of Missouri, Columbia, Missouri 65211, USA*

[2]*Geophysical Laboratory, Carnegie Institution of Washington, 5251 Broad Branch Road, NW Washington, District of Columbia 20015, USA*

[3]*HPSynC, Geophysical Laboratory, Carnegie Institution of Washington, Advanced Photon Source, Argonne National Laboratory, 9700 South Cass Avenue, Argonne, Illinois 60439, USA*

[4]*Department of Chemistry and INSTM, University of Pavia, Viale Taramelli 10-16, I-27100 Pavia, Italy*

(Received 15 April 2015; revised manuscript received 20 November 2015; published 13 January 2016)

We show that the pressure-induced metal-insulator transition (MIT) in $LaMnO_3$ is fundamentally different from the Mott-Hubbard transition and is percolative in nature, with the measured resistivity obeying the percolation scaling laws. Using the Gutzwiller method to treat correlation effects in a model Hamiltonian that includes both Coulomb and Jahn-Teller interactions, we show, one, that the MIT is driven by a competition between electronic correlation and the electron-lattice interaction, an issue that has been long debated, and two, that with compressed volume, the system has a tendency towards phase separation into insulating and metallic regions, consisting, respectively, of Jahn-Teller distorted and undistorted octahedra. This tendency manifests itself in a mixed phase of intermixed insulating and metallic regions in the experiment. Conduction in the mixed phase occurs by percolation and the MIT occurs when the metallic volume fraction, steadily increasing with pressure, exceeds the percolation threshold $v_c \approx 0.29$. Measured high-pressure resistivity follows the percolation scaling laws quite well, and the temperature dependence follows the Efros-Shklovskii variable-range hopping behavior for granular materials.

DOI: 10.1103/PhysRevB.93.024107

I. INTRODUCTION

The doped manganites such as $La_{1-x}Ca_xMnO_3$ are unique systems for studying competing interactions between spin, electronic, orbital, and lattice degrees of freedom [1–3]. The end member $LaMnO_3$ (LMO) is of special interest, since, while being governed by the same interactions, it is at the same time free from clutter due to the Ca dopants. The pressure-induced metal-insulator transition (MIT) in LMO has been long debated over two main issues. First, while resistance measurements indicate a sharp transition to the metallic state at the critical pressure $P_c \approx 32$ GPa [4], Raman measurements, on the other hand, show a gradual change with both Jahn-Teller (JT) distorted and undistorted regions persisting over a wide range of pressure [4–6]. An understanding of the MIT must explain this dual behavior, which we explain below in terms of percolation.

The second issue is the relative role of the competing interactions in mediating the MIT, namely bandwidth (W) and Hubbard U. Loa *et al.* [4] first suggested that the MIT is driven by bandwidth (W) enhancement with pressure, based on the fact that the JT distortion disappears much below P_c and therefore has no role to play, so that the change in U/W results in an MIT of the standard Mott-Hubbard type [7]. This conclusion was refuted by Baldini and Ramos and coworkers [5,6], who observed, to the contrary, that the distortions in fact persist beyond the MIT and remain relatively unchanged across the transition. Several theoretical studies [8–12] also suggested that JT interaction as well as the Coulomb coupling is important questioning the pure Mottness of the observed MIT. Trimarchi and Binggeli [8] studied the Mn-O distances under pressure with the Coulomb-corrected LDA + U density-functional method and found the Coulomb interaction to be essential in establishing the insulating ground state. Based on the dynamical-mean-field results (LDA + DMFT), Yamasaki *et al.* [9] argued that both the JT and the Coulomb interactions are important for the MIT. A similar conclusion was found from the slave-boson solution of a model Hamiltonian [11]. Yin *et al.* [10] suggested that the JT distortion is facilitated by the Coulomb U term via enhanced localization. Considering another aspect of the problem, Koch *et al.* [12] showed that in order to describe the orbital ordering seen in neutron scattering, the JT interactions are important, and the Kugel-Khomskii superexchange derived from the Coulomb U term is not sufficient for it. Much of this theory work was aimed at understanding the role of the competing interactions, rather than the phase coexistence across the MIT, although a recent hybrid-functional calculation [13] found different magnetic phases to be close in energy at $T = 0$, suggesting the propensity towards phase coexistence.

In this paper, from a Gutzwiller solution of a model Hamiltonian and high-pressure transport measurements, we show that the pressure-induced MIT in undoped LMO is percolative in nature. In other words, conducting transport does not occur as a result of the formation of a homogeneous metallic phase, as happens in the Mott-Hubbard MIT, but rather, it occurs when the volume fraction of the metallic region, gradually increasing with pressure, exceeds the percolation threshold. The overarching goal of our work is to demonstrate how percolation theory forms the foundation of the underlying physics of the MIT in LMO. We focus on the high-temperature paramagnetic phase, so that the transport is uncluttered by the magnetic transitions that exist at low temperatures.

*Present address: Instituto de Ciencia de Materiales de Madrid, CSIC, Cantoblanco, E-28049 Madrid, Spain.

II. MODEL HAMILTONIAN AND GUTZWILLER SOLUTION

We consider a two-band, spinless model Hamiltonian, containing the key Coulomb and JT interactions:

$$\mathcal{H} = \sum_{\langle ij\rangle,\alpha\beta} t_{ij}^{\alpha\beta}(\hat{c}_{i\alpha}^{\dagger}\hat{c}_{j\beta} + \text{H.c.}) - g\sum_{i}(Q_{i3}\hat{\sigma}_z + Q_{i2}\hat{\sigma}_x) + \frac{1}{2}K\sum_{i}(Q_{i3}^2 + Q_{i2}^2) + U\sum_{i}\hat{n}_{i1}\hat{n}_{i2}, \quad (1)$$

where $\hat{c}_{i\alpha}^{\dagger}$ creates an e_g electron in orbital α (= 1,2) at site i on the simple cubic Mn lattice with zero-pressure lattice constant a, $\vec{\sigma}$ is the pseudospin describing the two e_g orbitals, $|\uparrow\rangle = |x^2 - y^2\rangle$ and $|\downarrow\rangle = |z^2\rangle$, Q_2 and Q_3 are the two JT distortion modes of the MnO_6 octahedron, and K and U are the elastic constant for the JT modes and the intraorbital on-site Hubbard U Coulomb interaction, respectively. Only one spin is included in the Hamiltonian due to the following reason. Because of the large Hund's coupling $J_H \to \infty$, the e_g spins are always parallel to the core t_{2g} spins, with the result that the antiparallel spin states are altogether omitted due to their high energy. The two e_g states in the Hamiltonian, Eq. (1), therefore have their spins aligned with the local core spin, which can, however, vary from site to site.

Although the t_{2g} core spins are not explicitly included in the Hamiltonian, their effect on the hopping of the e_g electrons is a crucial part of the physics of the manganites and must be taken into account. The core spins modify the hopping integrals between the e_g electrons, since they are always aligned parallel with the core spins on each lattice site, via the Anderson-Hasegawa double exchange by the factor $\cos(\theta/2)$, where θ is the angle between two neighboring core spins, treated as classical [14]. As we are interested in the paramagnetic phase at room temperature, the random thermal fluctuations lead to the random fluctuations of the orientation of the core spins at each site, so that the thermal average of the Anderson-Hasegawa factor yields the result, $\langle\cos(\theta/2)\rangle = 2/3$, which modifies the hopping integral between the e_g electrons.

To describe the effect of pressure, we take the hopping integral to be volume dependent with $t^{\alpha\beta}(r) \propto r^{-7}$ following Harrison scaling [15], and add a Madelung term E_M and a repulsive interaction term E_R between the ions to keep the crystal from collapsing. The total energy then becomes $E = E_{\text{el}} + E_M + E_R$, and we have used the simplified forms $E_M = -A/r$, $E_R = B/r^{12}$, and as usual, $t^{\alpha\beta}$ may be expressed in terms of the $dd\sigma$ hopping integral, denoted here by $-t$. Guided by the literature [3,16–18], we set the parameters $A = 6$ eV, $B = 0.5$ eV, $g = 2.5$ eV/ Å, $K = 10\,\text{eV/Å}^2$, $U = 3$ eV, and $t = 0.6$ eV.

We have solved the model using the Gutzwiller approximation for the Coulomb interaction term in Eq. (1), treating the two e_g orbitals as pseudospins. The Gutzwiller wave function is given by

$$|\Psi_G\rangle = \eta^{\hat{D}}|\Psi_0\rangle, \quad (2)$$

where $|\Psi_0\rangle$ is the uncorrelated many-body wave function, $\hat{D}$ counts the site double occupancy, and the Gutzwiller variational parameter η is obtained by minimizing the expectation value of energy $\langle\Psi_G|\mathcal{H}|\Psi_G\rangle$. In the thermodynamic limit, the average double occupancy $d \equiv \langle\hat{D}\rangle$ is related to η by the expression $\eta^2 = 4d^2[(1-2d)^2 - m^2]^{-1}$ with $m = \langle\hat{n}_2 - \hat{n}_1\rangle$ being the orbital polarization. The electrons hop in a correlated manner, leading to a reduced kinetic energy, described by the Gutzwiller reduction factor [19,20],

$$\gamma(m,d) = \frac{2d(\sqrt{1-m-2d} + \sqrt{1+m-2d})^2}{1-m^2}, \quad (3)$$

valid for the half-filled case, viz., $n_1 + n_2 = 1$ corresponding to one e_g electron per site. A small d as compared to the uncorrelated value $d_{\text{uncorr.}} = n_1 n_2$ indicates a strongly correlated state and according to the Brinkman-Rice criterion [21], a Mott-Hubbard insulating ground state is indicated if $d \to 0$.

The band structure energy is computed by taking into account this reduction factor and diagonalizing the 2×2 Bloch Hamiltonian in the orbital space,

$$H_k = \begin{pmatrix} \varepsilon_{11}(k) - gQ_3 & \varepsilon_{12}(k) - gQ_2 \\ \varepsilon_{12}(k) - gQ_2 & \varepsilon_{22}(k) + gQ_3 \end{pmatrix}, \quad (4)$$

where $\varepsilon_{11}(k) = \bar{V}(\cos k_x a + \cos k_y a + 4\cos k_z a)/2$, $\varepsilon_{12}(k) = -\sqrt{3}\bar{V}(\cos k_x a - \cos k_y a)/2$, $\varepsilon_{22}(k) = 3\bar{V}(\cos k_x a + \cos k_y a)/2$, and $\bar{V} = -(2/3)\gamma(m,d)t(r)$, with $t(r) \propto r^{-7}$ and the factor 2/3 coming from the Anderson-Hasegawa renormalization as already discussed. We minimized the total energy per lattice site,

$$E = \sum_{\boldsymbol{k}\nu}^{\text{occ}} \varepsilon_{\boldsymbol{k}\nu}(d, Q_2, Q_3) + \frac{1}{2}KQ^2 + Ud + E_M + E_R, \quad (5)$$

as a function of d and Q_i for each volume, which yields the ground-state solution. Here $Q \equiv (Q_2^2 + Q_3^2)^{1/2}$ and $\varepsilon_{\boldsymbol{k}\nu}$ are the band structure energies obtained by diagonalizing the Hamiltonian H_k, Eq. (4).

III. THEORY RESULTS

The total energy, calculated from Eq. (5), is plotted in Fig. 1 for parameters corresponding to LMO as discussed earlier. It shows a double minimum as a function of volume corresponding to a JT distorted and an undistorted phase, indicating a phase separation in a range of volume shaded yellow in the figure. For volume constrained in the shaded region, the double minimum would imply the coexistence of two different phases: a high-volume insulating phase with volume V_2, and a low-volume metallic phase with volume V_1, with a sharp boundary between them. If pressure is fixed, then a first-order transition from the insulating to a metallic phase at a pressure corresponding to the common tangent would be implied. In the experiments, such a sharp transition is, however, not observed. For example, the equation of state shows a continuous change of volume with pressure [4].

The reason for the mixed phase, ubiquitous in the manganites, rather than a phase separation is a topic of considerable interest. A phase separated system could be energetically unfavorable due to multiple reasons, not included in our model. For example, the presence of a small amount of charged impurities because of unintentional doping could cause a deviation from charge neutrality of the two components and

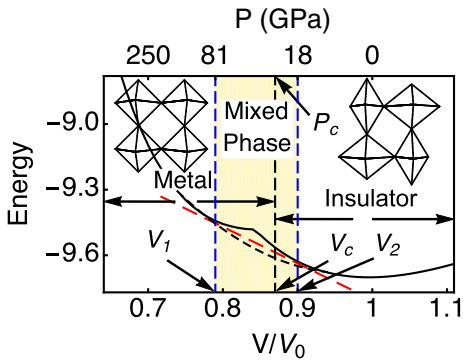

FIG. 1. Total energy as a function of volume obtained from Eq. (5) for parameters corresponding to LMO, indicating regions of JT distorted and undistorted phases. As volume is compressed below V_2, a metallic component begins to form, and the system conducts below V_c (black dashed line), when the metallic volume fraction v, calculated from the Maxwell-construction result, Eq. (6), exceeds the percolation threshold $v_c \approx 0.29$. The corresponding threshold pressure for MIT is $P_c \approx 31$ GPa as computed from the measured equation of state [4]. Energy is in units of t and volume is in units of V_0, the zero-pressure volume. The black dashed line (schematic) indicates the mixed phase region, if the phase separation is suppressed either due to interaction between the phases or for kinetic reasons (see text).

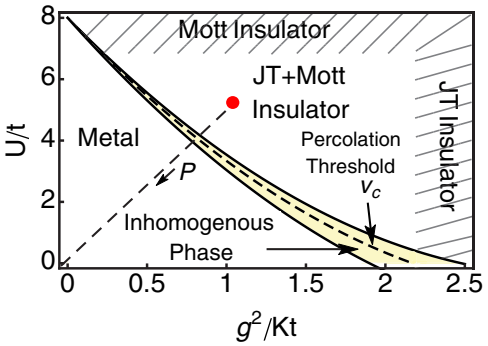

FIG. 2. Phase diagram showing the metallic and insulating regions, bridged by the inhomogeneous phase (shown in yellow). The system LMO, starting with the red dot at ambient pressure, moves along the dashed line as pressure is applied, first entering the inhomogeneous phase while still maintaining its insulating character, until the metallic fraction exceeds the percolation threshold v_c (curved dashed line). Finally, it crosses over to the fully metallic phase, where the metallic domains fill the entire volume.

would impede the formation of the phase separation due to the large cost in Coulomb energy. It would instead lead to a nanoscale inhomogeneous phase (or mixed phase) with intermixed metallic and insulating components (Coulomb frustrated phase separation) [22]. It has also been suggested that the mixed phase could even originate due to kinetic reasons, i.e., self-organized inhomogeneities resulting from a strong coupling between electronic and elastic degrees of freedom [23].

In fact, a number of experiments point to the existence of the mixed phase in LMO under pressure. These experiments include the Raman measurements [5,6], the continuous equation of state [4], as well as the present transport measurements. In particular, the Raman and the high-pressure resistivity measurements show that the metallic component slowly grows with pressure, while the equation of state indicates that no abrupt volume change occurs with pressure, which is consistent with the existence of the mixed phase. Even though the metallic fraction slowly grows with pressure, the transition to metallic conduction is, nevertheless, still sharp and occurs when the metallic fraction exceeds the percolation threshold.

The metallic fraction may be obtained from the Maxwell construction (red dashed line in Fig. 1). If $f_1(f_2)$ is the fraction of the substance in the metallic (insulating) phase in the mixed phase region ($V_1 < V < V_2$), V being the total volume, then we have the two equations: $f_1 + f_2 = 1$ and $f_1 V_1 + f_2 V_2 = V$, solving which we find the volume fraction of the metallic phase,

$$v \equiv \frac{f_1 V_1}{V} = \frac{V_2/V - 1}{V_2/V_1 - 1}. \tag{6}$$

The MIT occurs for $v > v_c \approx 0.29$, the percolation threshold, at which the metallic regions begin to touch and percolative conduction begins. We readily find from Eq. (6), the threshold volume for metallic conduction $V_c = (v_c/V_1 + (1 - v_c)/V_2)^{-1}$ and the corresponding P_c is found from the measured equation of state [4], and both are shown in Fig. 1.

Figure 2 summarizes the phase diagram, illustrating the competition between the Coulomb and the JT interactions. The phase diagram was calculated by starting with a fixed parameter set U, g, and t, e.g., the red dot in Fig. 2 corresponds to LMO at ambient pressure, and then by changing volume which scales these parameters. With decreasing volume (increasing pressure), the hopping integral t increases much more rapidly as compared to the other parameters (taken to be volume independent in our model), so that the system moves along the dashed line towards the origin as shown in the figure [if t doubles, then both U/t and $g^2/(Kt)$ are halved]. As the system traverses along the line, the volume changes and with it, the total energy, as shown in Fig. 1, from which the boundary of the inhomogeneous phase and the percolation threshold are determined. Figure 2 was obtained by studying the system traversing along a series of such lines in the parameter space.

The phase diagram, Fig. 2, shows distinct behaviors in different regions of the parameter space, viz., metallic behavior, insulating behavior driven by either correlation or Jahn-Teller interaction, or a mixed phase in the crossover region between the metal and insulator. For large Coulomb interaction, one gets a Mott-Hubbard insulator, while for a large JT coupling, one obtains a JT band insulator as a large gap opens up between the two orbitals due to a strong JT splitting.

The contrast between the Mott and the JT band insulator is illustrated in Fig. 3, where we have shown the change of the various quantities as the transition point is crossed. When g is zero or close to zero, we get the standard Mott-Hubbard MIT, in the sense that there is an abrupt change from the metallic state to the insulating state as U/t is increased beyond a critical value, and the system always remains in a single phase, either metallic or insulating. The Gutzwiller double occupancy d is zero at the MIT point, following the Brinkman-Rice criterion

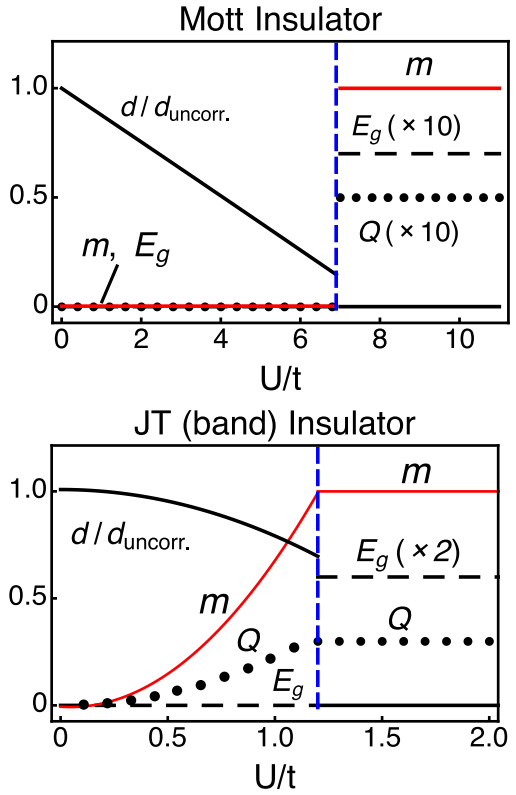

FIG. 3. Contrasting Mott insulator vs. JT band insulator. For weak JT coupling, $g^2/Kt = 0.04$ (top), the MIT is correlation-driven with the Gutzwiller double occupancy taking the Brinkman-Rice value $d \approx 0$ at the transition point, while in the opposite, strong-coupling limit, $g^2/Kt = 1.5$ (bottom), the MIT is driven by a large JT distortion Q, with d hardly changed from its uncorrelated value. In this figure, the system is assumed to be always in the homogeneous phase, so that the MIT corresponds to the kink in total energy like in Fig. 1 and not to the percolative MIT. Here, distortion Q is in Å, gap E_g is in units of t, m is the orbital polarization, and left of the blue line is a metal, while the right of it is an insulator.

[21]. On the other hand, if g is strong as compared to U, then correlation effects become negligible, and the MIT occurs because Q becomes large and the gap opens up because the energy separation between the two e_g orbitals, $2gQ$, becomes larger as compared to the bandwidth, leading to a JT band insulator. In this case, d does not change very much from its uncorrelated value as the MIT point is approached. At ambient pressure, LMO is in an intermediate regime, where the insulating state is formed by a combined effect of both Coulomb as well as JT interactions, as indicated by the red dot in Fig. 2.

IV. TRANSPORT MEASUREMENTS AND PERCOLATION LAWS

We have studied the mixed phase region experimentally from high-pressure transport measurements, which clearly shows the transport characteristic of an inhomogeneous (or mixed) phase with intermixed metallic and insulating regions. We measured the electrical resistance across the metal-

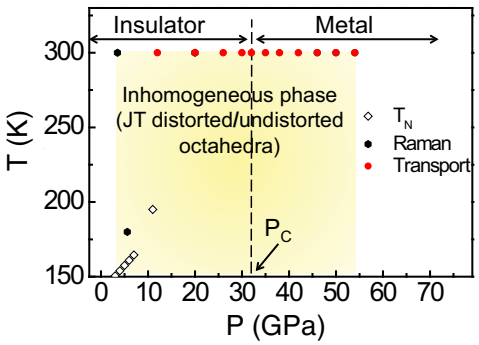

FIG. 4. Summary of the experimental high-temperature phase diagram. The observed inhomogeneous phase region is shaded yellow. The measured resistance corresponding to the red dots are shown in Fig. 5.

insulator transition region as a function of temperature and pressure up to 54 GPa.

In our experiments, samples of LMO were synthesized by solid-state reaction starting from 99.999% pure La_2O_3 and Mn_2O_3 and the oxygen stoichiometry was confirmed by thermo-gravimetric analysis. For the transport experiments, a miniature nonmagnetic diamond anvil cell was employed together with an Re gasket, previously insulated. The LMO powder was loaded in a 70-μm hole and four platinum leads (2-μm thick) were placed in electric contact with the sample to measure resistance in quasi-four-probe configuration using PPMS. At each pressure, resistance data were collected over cooling and warming temperature cycles (10–300 K) [24]. Pressure was measured using the ruby fluorescence technique. The resistance changed by five orders of magnitude as the pressure was varied across the MIT transition occurring at $P_c \approx 32$–35 GPa.

Figure 4 summarizes the high-temperature phase diagram, focusing on the paramagnetic region, which we have studied in the present work. The figure was constructed on the basis of the current experiment and earlier Raman [5] and Néel-temperature measurements [25].

Percolative conduction. The measured resistance corresponding to each transport data point, indicated by the red dots in Fig. 4, is shown in Fig. 5. The resistance shows percolative behavior characteristic of an inhomogeneous phase consisting of interspersed metallic and insulating puddles. Starting from an insulator at ambient pressure, the inhomogeneous phase sets in beyond $P \sim 3$ GPa, when the incipient metallic phase begins to appear and increases with pressure. Conducting transport occurs beyond $P_c \sim 32$ GPa, when the volume fraction of the metallic region exceeds the percolation threshold, roughly $v_c \approx 0.29$ [26]. At a much larger pressure P_M (theory predicts $P_M \sim 81$ GPa as seen from Fig. 1), the system would become a homogeneous single metallic phase; however, P_M is larger than our maximum pressure of 54 GPa and was not experimentally reached. The Raman data [5] show the presence of a mixture of distorted and undistorted regions across the MIT, specifically, up to the highest measured pressure of 34 GPa, while a remarkable decrease of the intensity-noise ratio in the Raman data at 32 GPa is a spectral signature of the onset of the MIT.

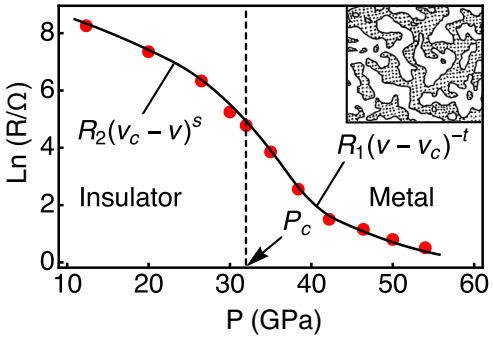

FIG. 5. Measured resistance in the paramagnetic phase ($T = 300K$) as a function of pressure showing percolative conduction in the mixed phase region. Close to the MIT, the resistance follows the percolation scaling laws, Eq. (7), with the critical exponents $t = 2.1 \pm 0.2$ and $s = 0.9 \pm 0.2$ and the fitted resistance constants $R_1 = 0.19\ \Omega$ and $R_2 = 5840\ \Omega$ (solid curve is a guide to the eye). The *inset* is a schematic of the inhomogeneous phase near the percolation threshold. The metallic volume fraction v was calculated by first computing the volume V for a given pressure from the experimental equation of state [4] and then using the Maxwell construction result, Eq. (6). The critical metallic fraction v_c, which corresponds to the critical pressure P_c, was similarly calculated.

The measured resistance, presented in Fig. 5, is described very well by the standard percolation scaling laws for the metal-insulator composites, viz.,

$$R = \begin{cases} R_1(v - v_c)^{-t} & v > v_c \text{ (metallic regime)} \\ R_1^{1-u} R_2^u & v = v_c \text{ (percolation threshold)} \\ R_2(v_c - v)^s & v < v_c \text{ (insulating regime),} \end{cases} \quad (7)$$

where v again is the metallic volume fraction, and $t = 1.6$–2.0, $s = 0.7$–1.0, and $u = t/(s + t)$ are universal critical exponents for three-dimensional (3D) percolation [27–29]. Our transport data (Fig. 5) were fitted to Eq. (7) by first computing the volume V for a given pressure using the equation of state [4] and then by finding the corresponding v from Eq. (6). The fitted critical exponents t and s (values listed in the Fig. 5 caption) are close to the theoretical exponents for 3D percolation, and the sigmoid shape of the transport curve closely resembles the same for the composite media [29].

The GEM equation for composites. Although a wide range of experimental results for conductor-insulator percolating systems and computer simulations can be fitted with the classic percolation equations expressed in Eq. (7), these equations are valid only in the limits where the conductivity of the metallic fillers tends to infinity, while the interspersed insulting matrix is a perfect insulator with the conductivity tending to zero. This is satisfied quite well in our case, as justified *a posteriori* from the fitted resistance ratio $R_2/R_1 \approx 3 \times 10^4$ (see Fig. 5 caption). In many composites, this condition is not satisfied quite so well. For these cases, McLachlan *et al.* [30] have proposed a phenomenological equation that has been successfully used to fit the conductivity data of such composites.

This so-called general effective medium (GEM) equation is in the form of an implicit equation for the resistance $R(v)$ as a function of the metallic volume fraction, which reads

$$\frac{(1 - v)\left(R^{1/s} - R_2^{1/s}\right)}{R^{1/s} + AR_2^{1/s}} + \frac{v\left(R^{1/t} - R_1^{1/t}\right)}{R^{1/t} + AR_1^{1/t}} = 0, \quad (8)$$

where $A = (1 - v_c)/v_c$ and R_1 and R_2 are, again, the resistances of the conductor and the insulator, respectively. This equation remains valid if the resistances are replaced by the corresponding resistivities. It can be easily verified that this single two-exponent percolation equation continuously interpolates between the three percolation equations in Eq. (7) and it reduces to a normalized form of each of them in the limits, $R_1 \to 0$ and $R_2 \to \infty$. In the crossover regime $v \approx v_c$ (more specifically, $|v - v_c| < (R_1/R_2)^{1/(t+s)}$), it reduces to the middle line of Eq. (7). We were able to fit our resistance data with this equation as well, which provided a single continuous curve, with the four fitting parameters R_1, R_2, t, and s. This fitting yielded very similar values to the parameters reported in Fig. 5, which were obtained by fitting the resistivity data to Eq. (7) in the limiting regions away from the critical region.

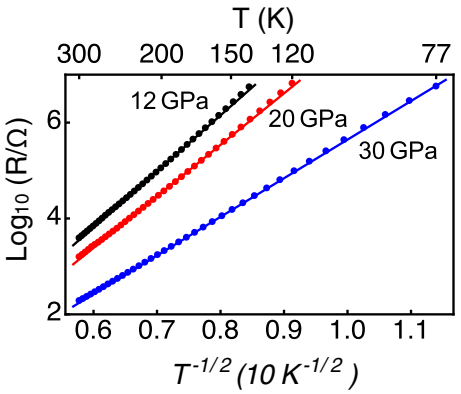

FIG. 6. The measured temperature dependence of resistance on the insulating side of the MIT at three different pressures.

Temperature dependence. The temperature dependence of the resistance in the insulating regime is shown in Fig. 6, which follows the Efros-Shklovskii variable range hopping (VRH) behavior [31,32],

$$R = R_0 \exp[(T_0/T)^{1/2}], \quad (9)$$

observed in a variety of granular materials [33], where nonpercolative metallic puddles (metallic fraction below the percolation threshold) are surrounded by insulating material.

V. CONCLUSION

In conclusion, we studied the metal-insulator transition in LMO under pressure using the Gutzwiller solution of a model Hamiltonian containing correlation and Jahn-Teller effects and high-pressure transport measurements. Our main result is that the MIT is driven by a combination of the correlation and Jahn-Teller effects, and it is percolative in nature, which is fundamentally different from the standard Mott-Hubbard transition. In the present case, the MIT occurs due to percolative conduction in a mixed phase consisting of interspersed metallic and insulation regions, while in the Mott-Hubbard transition, conduction occurs due to the sudden

change of the ground state of the system with some parameter, with the system maintaining a homogeneous, single phase across the MIT. The theory work showed that the system has a propensity for phase separation when volume is compressed, where the system separates into a metallic part and an insulating part divided by a single phase boundary. However, rather than the two parts forming two separate regions, they are interspersed among each other on the nanoscale in the experiment, thereby forming a mixed or an inhomogeneous phase (nanoscale phase separation). The exact reasons for this is unknown, but effects such as Coulomb interaction between the two parts or kinetic reasons have been proposed in the literature as discussed in the text.

The measured high-pressure resistance followed the percolation scaling laws both as a function of temperature and pressure, establishing the percolative nature of the metal-insulator transition. As pressure is applied on LMO, an insulator at $P = 0$, the metallic region begins to form around $P \sim 3$ GPa, with the metallic fraction gradually growing with pressure and eventually forming a conducting network beyond the percolation threshold, which occurs at $P_c \approx 32$ GPa. Thus, while the MIT is sharp, caused by the onset of the percolative conduction, there is no such sharp change in the metallic volume fraction, for it grows continuously across the MIT. In turn, since the metallic region contains undistorted JT octahedra, the average lattice distortion also changes continuously across the MIT as seen in the Raman data. The percolative MIT may be more common place in the oxide materials than is currently thought and needs further study, both from the viewpoints of fundamental science as well as of potential applications in oxide electronics.

ACKNOWLEDGMENTS

We thank P. Schlottmann and B. Shklovskii for helpful discussions. S.S. and M.S. were supported by the U.S. Department of Energy, Office of Science, under Grant No. DE-FG02-00ER45818. M.B. was supported as part of the Energy Frontier Research in Extreme Environments Center (EFree), an Energy Frontier Research Center funded by the U.S. Department of Energy, Office of Science under Grant No. DE-SC0001057.

[1] See for a review, E. Dagotto, *Nanoscale Phase Separations and Colossal Magnetoresistance*, Springer Series in Solid State Sciences Vol. 136 (Springer, New York, 2003).

[2] Y. Tokura and N. Nagaosa, Orbital Physics in Transition-Metal Oxides, Science **288**, 462 (2000).

[3] Z. Popović and S. Satpathy, Cooperative Jahn-Teller Coupling in the Manganites, Phys. Rev. Lett. **84**, 1603 (2000).

[4] I. Loa, P. Adler, A. Grzechnik, K. Syassen, U. Schwarz, M. Hanfland, G. Kh. Rozenberg, P. Gorodetsky, and M. P. Pasternak, Pressure-Induced Quenching of the Jahn-Teller Distortion and Insulator-to-Metal Transition in $LaMnO_3$, Phys. Rev. Lett. **87**, 125501 (2001).

[5] M. Baldini, V. V. Struzhkin, A. F. Goncharov, P. Postorino, and W. L. Mao, Persistence of Jahn-Teller Distortion up to the Insulator to Metal Transition in $LaMnO_3$, Phys. Rev. Lett. **106**, 066402 (2011).

[6] A. Y. Ramos, N. M. Souza-Neto, H. C. N. Tolentino, O. Bunau, Y. Joly, S. Grenier, J.-P. Itié, A.-M. Flank, P. Lagarde, and A. Caneiro, Bandwidth-driven nature of the pressure-induced metal state of $LaMnO_3$, Europhys. Lett. **96**, 36002 (2011).

[7] N. F. Mott, *Metal-Insulator Transitions*, 2nd ed. (Taylor & Francis, London, 1990).

[8] G. Trimarchi and N. Binggeli, Structural and electronic properties of $LaMnO_3$ under pressure: An *ab initio* LDA + U study, Phys. Rev. B **71**, 035101 (2005).

[9] A. Yamasaki, M. Feldbacher, Y.-F. Yang, O. K. Andersen, and K. Held, Pressure-Induced Metal-Insulator Transition in $LaMnO_3$ Is Not of Mott-Hubbard Type, Phys. Rev. Lett. **96**, 166401 (2006).

[10] W.-G. Yin, D. Volja, and W. Ku, Orbital Ordering in $LaMnO_3$: Electron-Electron versus Electron-Lattice Interactions, Phys. Rev. Lett. **96**, 116405 (2006).

[11] J. D. Fuhr, M. Avington, and B. Alascio, Pressure-Induced Insulator-Metal Transition in $LaMnO_3$: A Slave-Boson Approach, Phys. Rev. Lett. **100**, 216402 (2008).

[12] E. Pavarini and E. Koch, Origin of Jahn-Teller Distortion and Orbital Order in $LaMnO_3$, Phys. Rev. Lett. **104**, 086402 (2010).

[13] J. He, M.-X. Chen, X.-Q. Chen, and C. Franchini, Structural transitions and transport-half-metallic ferromagnetism in $LaMnO_3$ at elevated pressure, Phys. Rev. B **85**, 195135 (2012).

[14] P. W. Anderson and H. Hasegawa, Considerations on Double Exchange, Phys. Rev. **100**, 675 (1955); P.-G. De Gennes, Effects of Double Exchange in Magnetic Crystals, *ibid.* **118**, 141 (1960).

[15] W. A. Harrison, *Electronic Structure and the Properties of Solids* (Freeman, San Francisco, 1980).

[16] S. Satpathy, Z. S. Popović, and F. R. Vukajlović, Electronic Structure of the Perovskite Oxides: $La_{1-x}Ca_xMnO_3$, Phys. Rev. Lett. **76**, 960 (1996); W. E. Pickett and D. J. Singh, Electronic structure and half-metallic transport in the $La_{1-x}Ca_xMnO_3$ system, Phys. Rev. B **53**, 1146 (1996).

[17] A. J. Millis, Cooperative Jahn-Teller effect and electron-phonon coupling in $La_{1-x}A_xMnO_3$, Phys. Rev. B **53**, 8434 (1996).

[18] G. D. Tang, S. P. Liu, X. Zhao, Y. G. Zhang, D. H. Ji, Y. F. Li, W. H. Qi, W. Chen, and D. L. Hou, Study of the free energy of the $La_{1-x}Ca_xMnO_3$ manganites based on the temperature dependence of the crystal cell volume, Appl. Phys. Lett. **95**, 121906 (2009).

[19] M. C. Gutzwiller, Effect of Correlation on the Ferromagnetism of Transition Metals, Phys. Rev. Lett. **10**, 159 (1963); Effect of Correlation on the Ferromagnetism of Transition Metals, Phys. Rev. **134**, A923 (1964); Correlation of Electrons in a Narrow *s* Band, **137**, A1726 (1965).

[20] M. Sherafati and S. Satpathy, Gutzwiller variational method for intersite Coulomb interactions: The spinless fermion model in one dimension, Phys. Rev. B **88**, 035114 (2013).

[21] W. F. Brinkman and T. M. Rice, Application of Gutzwiller's Variational Method to the Metal-Insulator Transition, Phys. Rev. B **2**, 4302 (1970).

[22] V. B. Shenoy, T. Gupta, H. R. Krishnamurthy, and T. V. Ramakrishnan, Coulomb Interactions and Nanoscale Electronic

Inhomogeneities in Manganites, Phys. Rev. Lett. **98**, 097201 (2007).

[23] K. H. Ahn, T. Lookman, and A. R. Bishop, Strain-induced metal-insulator phase coexistence in perovskite manganites, Nature (London) **428**, 401 (2004).

[24] For further experimental details, see, M. Baldini, T. Muramatsu, M. Sherafati, H. Mao, L. Malavasi, P. Postorino, S. Satpathy, and V. V. Struzhkin, Origin of colossal magnetoresistance in $LaMnO_3$ manganite, Proc. Natl. Acad. Science **112**, 10869 (2015).

[25] J.-S. Zhou, Y. Uwatoko, K. Matsubayashi, and J. B. Goodenough, Breakdown of magnetic order in Mott insulators with frustrated superexchange interaction, Phys. Rev. B **78**, 220402 (2008).

[26] Assuming the metallic region to consist of randomly packed spheres of radius r, the volume fraction for the onset of percolation is given by $v_c \approx 0.29$ and is independent of r. See, e.g., G. E. Pike and C. H. Seager, Phys. Rev. B **10**, 1421 (1974).

[27] D. Stauffer and A. Aharony, *Introduction to Percolation Theory*, 2nd ed. (Taylor & Francis, London, 1998).

[28] D. J. Bergman and D. Stroud, Physical Properties of Macroscopically Inhomogeneous Media, in *Solid State Physics: Advances in Research and Applications*, edited by H. Ehrenreich and D. Turnbull (Academic Press, San Diego, 1992), Vol. 46, pp. 147–269.

[29] C.-W. Nan, Physics of inhomogeneous inorganic materials, Prog. Mat. Sci. **37**, 1 (1993).

[30] D. S. McLachlan, M. Blaszkiewicz, and R. E. Newnham, Electrical resistivities of the composites, J. Am. Ceram. Soc. **73**, 2187 (1990); D. S. McLachlan and G. Sauti, The AC and DC Conductivity of Nanocomposites, J. Nanomater. **2007**, 30389 (2007).

[31] A. L. Efros and B. I. Shklovskii, Coulomb gap and low temperature conductivity of disordered systems, J. Phys. C **8**, L49 (1975); Critical Behaviour of Conductivity and Dielectric Constant near the Metal-Non-Metal Transition Threshold, Phys. Stat. Sol. **76**, 475 (1976).

[32] B. Skinner, T. Chen, and B. I. Shklovskii, Theory of hopping conduction in arrays of doped semiconductor nanocrystals, Phys. Rev. B **85**, 205316 (2012); J. Zhang and B. I. Shklovskii, Density of states and conductivity of a granular metal or an array of quantum dots, *ibid.* **70**, 115317 (2004).

[33] For a review, see I. S. Beleborodov, A. V. Lopatin, V. M. Vinokur, and K. B. Efetov, Granular electronic systems, Rev. Mod. Phys. **79**, 469 (2007).